

# Application of two segmentation protocols during the processing of virtual images in rapid prototyping: ex vivo study with human dry mandibles

Eduardo Gomes Ferraz · Lucio Costa Safira Andrade ·  
Aline Rode dos Santos · Vinicius Rabelo Torregrossa ·  
Izabel Regina Fischer Rubira-Bullen ·  
Viviane Almeida Sarmento

Received: 11 September 2012 / Accepted: 9 January 2013 / Published online: 24 January 2013  
© Springer-Verlag Berlin Heidelberg 2013

## Abstract

**Objectives** The aim of this study was to evaluate the accuracy of virtual three-dimensional (3D) reconstructions of human dry mandibles, produced from two segmentation protocols (“outline only” and “all-boundary lines”).

E. G. Ferraz · L. C. S. Andrade · A. R. dos Santos ·  
V. R. Torregrossa · V. A. Sarmento (✉)  
School of Dentistry, Federal University of Bahia,  
Avenida Araújo Pinho, n. 62 Canela,  
41110-150 Salvador, Bahia, Brazil  
e-mail: viviane.sarmiento@gmail.com

E. G. Ferraz  
e-mail: ed\_ferraz@yahoo.com.br

L. C. S. Andrade  
e-mail: lucio.safira@ig.com.br

A. R. dos Santos  
e-mail: aline.rode@yahoo.com.br

V. R. Torregrossa  
e-mail: vinicius.torregrossa@bol.com.br

I. R. F. Rubira-Bullen  
School of Dentistry, State University of São Paulo-Bauru,  
Alameda Doutor Octavio Pinheiro Brisolla,  
n. 9-75, Vila Universitária,  
17012-101 Bauru, São Paulo, Brazil  
e-mail: izrubira@fob.usp.br

V. A. Sarmento  
School of Dentistry, State University of Feira de Santana,  
Avenida Transnordestina, s/n, Novo Horizonte,  
44036-900 Feira de Santana, Bahia, Brazil

**Materials and methods** Twenty virtual three-dimensional (3D) images were built from computed tomography exam (CT) of 10 dry mandibles, in which linear measurements between anatomical landmarks were obtained and compared to an error probability of 5 %.

**Results** The results showed no statistically significant difference among the dry mandibles and the virtual 3D reconstructions produced from segmentation protocols tested ( $p=0,24$ ).

**Conclusions** During the designing of a virtual 3D reconstruction, both “outline only” and “all-boundary lines” segmentation protocols can be used.

**Clinical relevance** Virtual processing of CT images is the most complex stage during the manufacture of the biomodel. Establishing a better protocol during this phase allows the construction of a biomodel with characteristics that are closer to the original anatomical structures. This is essential to ensure a correct preoperative planning and a suitable treatment.

**Keywords** X-ray computed tomography · Computer-assisted image processing · Three-dimensional imaging · Rapid prototyping

## Introduction

Rapid prototyping (RP) is a technology that allows the construction of a physical model with the same geometric characteristics as the original model, using CAD/CAM (computer-aided design/computer-aided manufacturing) technology [1–5]. There are many applications of both of these models found in an industry where the prototypes

often precede the mass production of a particular piece. In health care, the models are called biomodels, and they assist in the planning and simulation of different procedures, thereby making the results more predictable [6–10].

Conversion of two-dimensional images (2D) obtained by computed tomography (CT) into three-dimensional (3D) images is performed with specific medical software with several electronic tools. The evaluation of these processes is crucial for the construction of biomodels that adequately reproduce the patient's anatomy, and therefore can ensure that the process performed on the biomodels be safely implemented in their surgical planning and rehabilitation [11–15]. One of the most important stages is the image segmentation, which is characterized by the separation of the structures to be represented in the biomodel. This process is done from the definition of a range of grayscale voxel that expresses only the voxels in the region of interest, which is called the threshold value [16, 17]. The segmentation of medical images is a difficult process, mainly due to overlapping intensities, anatomical complexity, and variability in shape and size, in addition to the usual limitations in the imaging equipment or input data, such as noise perturbations, intensity inhomogeneities, partial volume effect, and low contrast [18, 19].

Some studies in the literature [20, 21] point out that determining the range of threshold is empiric and does not comply with specific standards. The 3D Doctor® software (Able Corporation, USA) offers three different types of segmentation: “outline only,” “all-boundary lines,” and “skeleton boundary.” The outline only option should only be used to target the profile of the structure of interest. In this case, no cavities, openings, or islands are visible. The all-boundary lines option targets all possible limits of the structure, including regions with holes and islands. The skeleton boundary option allows only the segmentation of the skeleton of the region of interest [22]. Consequently, the determination of the threshold depends on prior knowledge of the grayscale voxel of the structure in question by the software operator [21].

This study aims to verify the accuracy of virtual 3D reconstructions of human dry mandibles, produced with two segmentation protocols (“outline only” and “all-boundary lines”).

## Materials and methods

This study was approved by Ethics in Research Committee of the Dentistry School, Federal University of Bahia (CAEE 0019.368.000-08). Ten human dry mandibles were randomly selected. Criteria for inclusion were that mandibles should be intact, regardless of whether or not the teeth were present, and if teeth were present there were no metallic

restorations or prosthesis. All dry mandibles were subjected to helical CT (Elscent-Twin Flash CT, USA). Each mandible was placed on the table of the tomographic apparatus on a styrofoam platform and fastened with tape to simulate the real position of an examination *in vivo*. There were obtained axial slices parallel to mandible base with 1.1-mm thickness, 1-mm increment, and pitch of 1.5. The field of view used was less than 250 mm and without tilting the gantry. The entire height of the mandible was scanned, with a margin of 1.5 cm above and below the area of interest. The images in DICOM (Digital Imaging and Communications in Medicine) format were archived on CD-ROM.

## Virtual processing of images

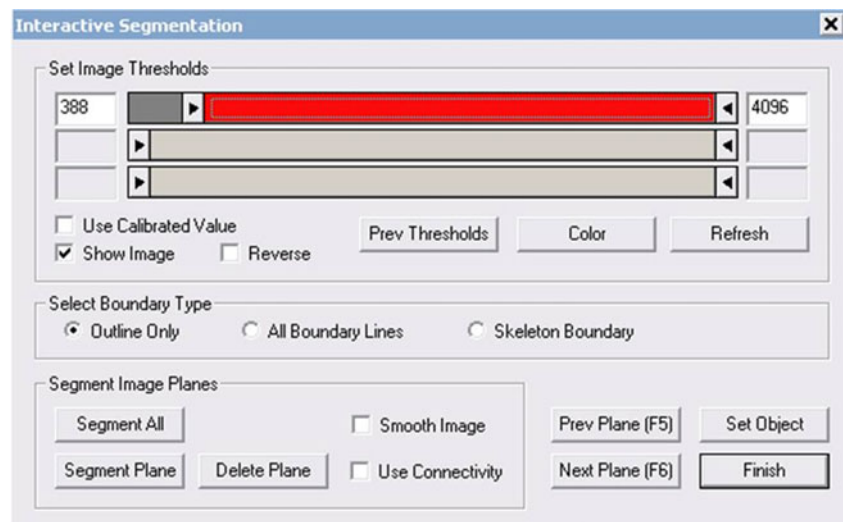
3D Doctor® software was used to make virtual 3D reconstructions. Segmentation of the images was performed to determine the values of grayscale voxels that corresponded to the anatomical structures of interest using the tool “Interactive Segmentation to Generate Object Boundaries”. By selecting this tool, the program automatically determines the lower and upper grayscale voxel. In this study, we chose to accept the lower limit of the grayscale voxel, provided by the software; the upper limit set by the operator was always the maximum of the scale (value 4,096 HU) (Fig. 1). The type of segmentation (“outline only” or “all-boundary lines”) was chosen from the tool “Select Boundary Type”.

First, the outline only option was selected to target only the profile of the structure of interest (Fig. 2). The accuracy of this process was given for each axial image separately. Subsequently, the virtual 3D reconstructions were generated by using the “Complex Surface Rendering” method and were subsequently saved as STL format. Thus, 10 virtual 3D reconstructions were obtained from “outline only” segmentation protocol. The entire procedure described above was repeated with the “all-boundary lines” option selected; this allowed for the inclusion of all possible limits of the structure, including those with holes and islands (Fig. 3). Thus, 10 virtual 3D reconstructions were obtained from “all-boundary lines” segmentation protocol and then archived. A total of 20 3D reconstructions obtained after virtual processing, previously stored as STL format, were renamed by an external observer, so that during the anatomic measurements, the examiner would have no knowledge of the segmentation protocol used to originate the virtual 3D reconstruction.

## Measurements

Each virtual 3D reconstruction was viewed in the 3D Doctor® software, and the linear measurements between

**Fig. 1** Segmentation of the image. The maximum value (4,096 HU) of the sliderbar was selected



anatomical landmarks, as described in Table 1, were made. The measurements on the virtual 3D reconstructions were performed using the “measure distance tool” of the software. The anatomical measurements were also performed on the original dry mandibles using a high-precision digital caliper (Series 727; Starrett® Industria e Comercio Ltda, Itu, São Paulo). All measurements were performed by three observers, twice each, with a minimum interval of 1 week between measurements. The 1,440 measurements were noted in specific worksheets in Microsoft Excel® for further statistical analysis. Lin’s concordance was used to evaluate the intra- and intercoefficient of correlation. The Kolmogorov–Smirnov test was used to check for normal distribution in each group. As the distribution did not follow the normal curve, we applied the nonparametric Friedman test with a probability of error of 5 %.

## Results

After applying Lin’s concordance test, the intraobserver variability of observer 1 was 0.99, 0.98 for observer 2, and 0.98 for observer 3. This indicates an extremely strong correlation, demonstrating the reproducibility of the method. Then, the second evaluations by each of the examiners were compared to establish the interobserver variability. Lin’s concordance test demonstrated that the correlation coefficient was 0.97 between observers 1 and 2, 0.98 between observers 1 and 3, and 0.98 between observers 2 and 3. This demonstrates once again a very strong agreement, confirming the calibration of the examiners. We used only the data measured by observer 1 for statistical analysis. No statistical difference was observed among the groups ( $p=0.24$ ). The data are displayed in Table 2.

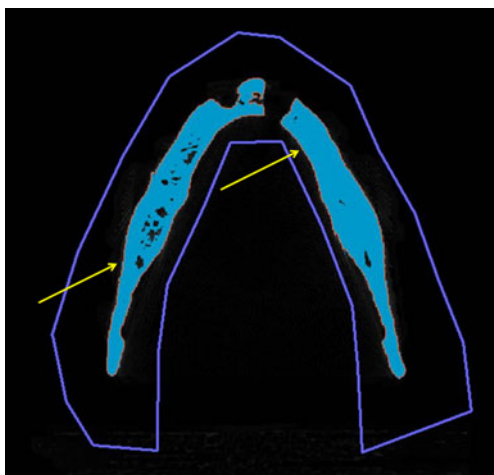


**Fig. 2** “Outline only” segmentation. The yellow arrows point to the red line, traced only on the structure of interest

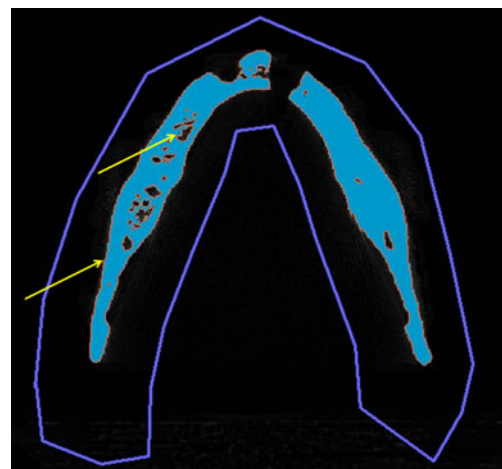


**Fig. 3** “All-boundary lines” segmentation. The yellow arrows point to the red line, traced on all possible limits of the structure, including regions with holes and islands

**Table 1** The anatomic measurements

Anatomic measurement	Definition
Height of mandibular symphysis	Distance between the topmost point in the midline of the alveolar process to the base of the mandible
Distance between mental foramina	Selection of the more anterior point of the mental foramen
Height of the right mental foramen	Distance between the point located in the center right of the mental foramen to the lowest point of the mandibular base
Height of the left mental foramen	Distance between the point located in the center left of the mental foramen to the lowest point of the mandibular base
Height of the right mandible	Distance between the lowest point of the mandibular notch to the lowest point of the base of the mandible on the right side
Height of the left mandible	Distance between the lowest point of the mandibular notch to the lowest point of the base of the mandible on the left side
Distance between the region of the mandibular symphysis and the angle of the mandible on the right side	Selecting the most anterior point of the mandibular symphysis at a right angle to the jaw
Distance between the region of the mandibular symphysis and the angle of the mandible on the left side	Selecting the most anterior point of the mandibular symphysis at a right angle to the jaw

## Discussion

Virtual processing of the acquired images is a decisive step in biomodeling. This study has evaluated the effect of two segmentation protocols (“outline only” and “all-boundary lines”) for rendering virtual of 3D reconstructions, from a comparison of eight linear measurements made in dry mandibles and on their respective virtual 3D reconstructions. It had used two different tools of the 3D Doctor software,

**Table 2** Comparison of the linear measurements of dry mandibles and 3D virtual reconstructions, according the segmentation protocol

Segmentation protocol of virtual models	Median		Difference (mm)	<i>p</i> value
	Virtual models (mm)	Dry mandible (mm)		
“Outline only”	37.70	35.40	2.30	0.24
“All-boundary lines”	37.48	35.40	2.08	

although there is also a third tool available (“skeleton boundary”). These two segmentation tools were selected because during the construction of 3D virtual models, these images were more similar to the dry mandibles when compared with those generated by the “skeleton boundary” tool.

The results of this study showed no statistical differences among the groups ( $p=0.24$ ), as shown in Table 2. These results show that although the two segmentation tools have unique characteristics, the “outline only” protocol, which checks the lines outside the image, and the “all-boundary lines” protocol, which shows a selection of internal and external lines of the image, can be used during the construction of virtual models without any change in the outcome. This indicates that the two segmentation protocols evaluated are capable of producing biomodels with excellent quality and, thus, providing safe surgical procedures and adequate functional and esthetic results in patients using this technology.

Segmentation is characterized by a process of separating the data from a given region that will be used in the reconstruction of a surface [23–25]. Several factors may influence the accuracy of segmentation, such as the irregular distribution of points, image noise, and insufficient information on the limits and complexity of the surface shape of the structure [23]. Several forms of segmentation or determining the threshold of the image (the intensity of the grayscale voxel that comprise the biomodel) should be evaluated because they could affect the dimensions of virtual 3D reconstructions generated. This step determines the limits of the model, its shape and characteristics, representing a crucial step in the processing of virtual 3D reconstructions [21]. In vivo, segmentation eliminates images of soft tissue, leaving only bone tissue; it can even delete metallic artifacts produced by CT when the patient has metal parts, such as prosthesis or dental restorations [11, 12, 26]. This is particularly important in dentistry because the region to be plotted is often affected by artifacts of this nature. In this study, the dry mandibles with teeth had no fillings or metal prosthesis, ensuring that the virtual models did not present artifacts. This has reduced the manual editing of the slices during 3D reconstruction.

The image segmentation obtained from a scanner or magnetic resonance imaging (MRI) is a difficult task because of the complexity and size of internal structures [27]. Furthermore, the shape of the structure interferes with the process of segmentation because the depth of the concavity of a structure directly affects the boundaries of the region. Thus, having prior knowledge of the regions with concavity, along with other relevant information, is important in this process [23]. For determining of the threshold value, the software displays a scale and the operator can then determine the range to obtain adequate representation. If the region of choice is bone tissue, a higher threshold value can be selected to remove any soft tissue areas [16, 17].



Determining the threshold value influences on the dimension of structures of interest is an important part of the process, for example, when the virtual 3D reconstructions present fine structures, such as the orbital cavity. If higher threshold values are selected, these structures will be not included in the bio-models. In these cases, some authors have suggested selecting lower threshold values. Thus, when structures with high density, such as cortical bone, are larger than the size of the voxel, the surfaces are well-defined and contain easily recognized transitions [28]. However, for a low-density structure, such as the trabecular bone, its representation will occupy only a portion of the voxel and the details will be suppressed by not exceeding the threshold value [16].

Kragstkov et al. [20], when comparing the accuracy of the techniques with biomodel stereolithography and selective laser sintering, discovered a variation in the precision of the measurements between 0.5 and 0.1 mm. One of the possible causes of these changes is a partial volume effect of CT and empirical determination of the threshold value.

Although it seems like a simple task, in practice, segmentation is important for the successful implementation of the process because, if the range of grayscale voxel is determined inappropriately, there is a thickening or thinning of the bone structures of interest and a possible change in the biomodel dimensions. The subjectivity of the process lies in the fact that the determination of the threshold depends upon the software operator having prior knowledge of the grayscale voxel of the structure in question [21].

Hieu et al. [1] assessed the thickness of the skull from the determination of different threshold values in the Mimics® software and observed that at a value of 200 HU, the skull thickness was 6.64 mm, whereas at the threshold value of 500 HU, a measurement of 5.52 mm was obtained, with a difference of 1.12 mm in the average thickness. Thus, the authors concluded that the determination of an optimal threshold value depends mainly on the purpose of the construction and its manufacture, as well as the surgeon's clinical requirement. Moreover, to ensure that the virtual model is correct and accurate, it is necessary to compare it directly with data from the CT/MRI of the patient.

Some studies in the literature [7, 21, 29, 30] have evaluated the accuracy of different methods of RP of the skulls, jaws, and other bones, without soft tissue. In this study, the soft tissues were not simulated because we did not intend to include another error source. To erase the soft tissues of the mandible during the processing of the images is necessary to apply the segmentation tool, but this phase is subjective and may add differences among the reconstructions [31].

This care was observed in our study, in which the images were from dry mandibles (containing no soft tissue); therefore, the segmentation of the images was facilitated by the absence of potential failures, validating the choice of the lower limit of the grayscale provided

automatically by the software. In vivo, this phase may be responsible for any discrepancies, which cannot be assessed in this study.

In general, determining the range of threshold is empiric and does not obey specific standards [20, 21]. Therefore, it is possible to produce errors in the biomodel if the software is not properly adjusted or if the operator does not have enough experience or deep knowledge of human anatomy. The making of virtual 3D reconstructions is complex, especially during the image segmentation, and additional studies are required to explore other methods for establishing better protocols.

## Conclusion

In conclusion, according to the results of this study, the virtual models made using “outline only” or “all-boundary lines” protocols showed no significant differences in dimensions compared to the original dry mandibles. It should be emphasized, however, that variables such as the presence of soft tissues, or metal fillings, or even operator background were not included in the current study, which should be investigated in further research. This allows inferring that biomodels constructed from segmentation protocols evaluated can be reliable and ensure adequate results in surgical planning and treatment of patients.

**Acknowledgments** The authors thank Research Support Foundation of the State of Bahia.

**Conflict of interest** The authors declare that they have no conflict of interest.

## References

1. Hieu LC, Zlatov N, Sloten FV, Bohez E, Khanh L, Binh PH, Oris P, Toshev Y (2005) Medical rapid prototyping applications and methods. *Assem Autom* 25:284–292
2. Singare S, Yaxiong L, Dichen L, Bingheng L, Sanhu H, Gang L (2006) Fabrication of customised maxillo-facial prosthesis using computer-aided design and rapid prototyping techniques. *Rapid Prototyp J* 12:206–213
3. Hu YJ, Hardianto A, Li SY, Zhang ZY, Zhang CP (2007) Reconstruction of a palatomaxillary defect with vascularized iliac bone combined with a superficial inferior epigastric artery flap and zygomatic implants as anchorage. *Int J Oral Maxillofac Surg* 36:854–857
4. Li WZ, Zhang MC, Li SP, Zhang LT, Huang Y (2009) Application of computer-aided three-dimensional skull model with rapid prototyping technique in repair of zygomatico-orbito-maxillary complex fracture. *Int J Med Robot Comput Assist Surg* 5:158–163
5. Pattnaik S, Karunakar DB, Jha PK (2012) Developments in investment casting process—a review. *J Mater Process Tech* 212:2332–2348

6. Liu GH, Wong YS, Zhang YF, Loh HT (2002) Error-based segmentation of cloud data for direct rapid prototyping. *Comput Aided Des* 35:633–645
7. Meakin JR, Shepherd DET, Hukins DWL (2004) Fused deposition models from CT scans. *Br J Radiol* 77:504–507
8. Hassan B, Souza PC, Jacobs R, Berti AS, van der Stelt P (2010) Influence of scanning and reconstruction parameters on quality of three-dimensional surface models of the dental arches from cone beam computed tomography. *Clin Oral Invest* 14:303–310
9. Turgut G, Sacak B, Kiran K, Bas L (2009) Use of rapid prototyping in prosthetic auricular restoration. *J Craniofac Surg* 20:321–325
10. Bibb R, Winder J (2010) A review of the issues surrounding three-dimensional computed tomography for medical modelling using rapid prototyping techniques. *Radiography* 16:78–83
11. Winder J, Bibb R (2005) Medical rapid prototyping technologies: state of the art and current limitations for application in oral and maxillofacial surgery. *J Oral Maxillofac Surg* 63:1006–1015
12. Robiony M, Salvo I, Costa F, Zerman N, Bazzocchi M, Toso F, Bandera C, Filippi S, Felice M, Politi M (2007) Virtual reality surgical planning for maxillofacial distraction osteogenesis: the role of reverse engineering rapid prototyping and cooperative work. *J Oral Maxillofac Surg* 65:1198–1208
13. Gao H, Chae O (2010) Individual tooth segmentation from CT images using level set method with shape and intensity prior. *Pattern Recognit* 43:2406–2417
14. Kato A, Ohno N (2009) Construction of three-dimensional tooth model by micro-computed tomography and application for data sharing. *Clin Oral Invest* 13:43–46
15. Wang C, Wang WA, Lin M (2010) STL rapid prototyping bio-CAD model for CT medical image segmentation. *Comput Ind* 61:187–197
16. Liu Q, Leu MC, Schmitt SM (2006) Rapid prototyping in dentistry: technology and application. *Int J Adv Manuf Technol* 29:317–335
17. Singare S, Dichen L, Bingheng L, Yanpu L, Zhenyu G, Yaxiong L (2004) Design and fabrication of custom mandible titanium tray based on rapid prototyping. *Med Eng Phys* 26:671–676
18. Del Fresno M, Vénere M, Clausse A (2009) A combined region growing and deformable model method for extraction of closed surfaces in 3D CT and MRI scans. *Comput Med Imag Graph* 33:369–376
19. Lai HC, Chang YH, Lai JY (2009) Development of feature segmentation algorithms for quadratic surfaces. *Adv Eng Softw* 40:1011–1022
20. Kragsskov J, Sindet-Pedersen S, Gyldensted C, Jensen KL (1996) A comparison of three-dimensional computed tomography scans and stereolithographic models for evaluation of craniofacial anomalies. *J Oral Maxillofac Surg* 54:402–411
21. Choi JY, Choi JH, Kim NK, Kim Y, Lee JK, Kim MK, Lee JH, Kim MJ (2002) Analysis of errors in medical rapid prototyping models. *Int J Oral Maxillofac Surg* 31:23–32
22. Able Software Corp (2006) 3D-Doctor: 3D-imaging, modeling, rendering and measurement software. Version 4.0. User's manual, Lexington
23. Lai YK, Hua SM, Martin RR, Rosin PL (2009) Rapid and effective segmentation of 3D models using random walks. *Comput Aided Geo Des* 26:665–679
24. Razdan A, Bae M (2003) A hybrid approach to feature segmentation of triangle meshes. *Comput Aided Des* 35:783–789
25. Mallepree T, Bergers D (2009) Accuracy of medical RP models. *Rapid Prototyp J* 15:325–332
26. Scarfe WC, Farman AG, Sukovic P (2006) Clinical applications of cone-beam computed tomography in dental practice. *J Can Dent Assoc* 72:75–80
27. Provot L, Debled-Rennesson I (2009) 3D noisy discrete objects: segmentation and application to smoothing. *Pattern Recog* 42:1626–1636
28. Schneider J, Decker R, Kalender WA (2002) Accuracy in medical modeling. *Phidias Rapid Prototyp Med* 8:5–14
29. Waitzman AA, Posnick JC, Armstrong DC, Pron GE (1992) Craniofacial skeletal measurements based on computed tomography: part I. Accuracy and reproducibility. *Cleft Palate Craniofac J* 29:112–117
30. Asaumi J, Kawai N, Honda Y, Shigehara H, Wakasa T, Kishi K (2001) Comparison of three-dimensional computed tomography with rapid prototype models in the management of coronoid hyperplasia. *Dentomaxillofac Radiol* 30:330–335
31. Ferraz EG, Andrade LCS, Santos AR, Torregrossa VR, Freire MRS, Sarmiento VA (2011) Effect of different surface processing protocols in three-dimensional images for rapid prototyping. *Adv Eng Softw* 42:332–335

Copyright of Clinical Oral Investigations is the property of Springer Science & Business Media B.V. and its content may not be copied or emailed to multiple sites or posted to a listserv without the copyright holder's express written permission. However, users may print, download, or email articles for individual use.